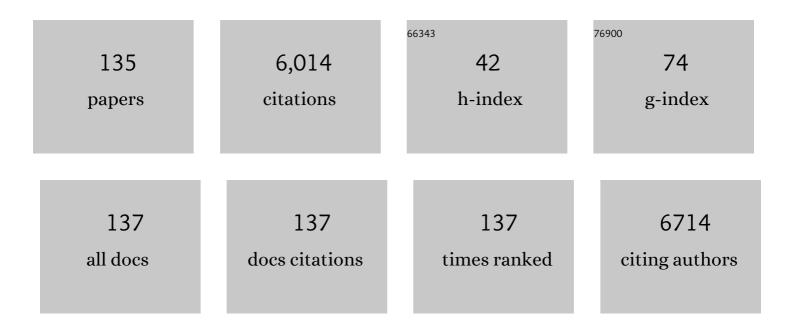
David Dean

List of Publications by Year in descending order

Source: https://exaly.com/author-pdf/2977862/publications.pdf Version: 2024-02-01



#	Article	IF	CITATIONS
1	Chemical Polishing of Additively Manufactured, Porous, Nickel–Titanium Skeletal Fixation Plates. 3D Printing and Additive Manufacturing, 2022, 9, 269-277.	2.9	16
2	Craniofacial and Dental Tissue. , 2022, , 287-310.		0
3	Chaotic printing of hydrogel carriers for human mesenchymal stem cell expansion. Procedia CIRP, 2022, 110, 236-241.	1.9	0
4	The mechanical reliability of vat photopolymerization 3D printing of isosorbide-derived polyester porous tissue engineering scaffolds Procedia CIRP, 2022, 110, 117-121.	1.9	1
5	Biological and Corrosion Evaluation of In Situ Alloyed NiTi Fabricated through Laser Powder Bed Fusion (LPBF). International Journal of Molecular Sciences, 2021, 22, 13209.	4.1	5
6	Photocrosslinking-based 3D printing of unsaturated polyesters from isosorbide: A new material for resorbable medical devices. Bioprinting, 2020, 18, e00062.	5.8	17
7	Biocompatibility of a novel heat-treated and ceramic-coated magnesium alloy (Mg–1.2Zn–0.5Ca–0.5Mn) for resorbable skeletal fixation devices. MRS Communications, 2020, 10, 467-474.	1.8	6
8	Design, Modeling, Additive Manufacturing, and Polishing of Stiffness-Modulated Porous Nitinol Bone Fixation Plates Followed by Thermomechanical and Composition Analysis. Metals, 2020, 10, 151.	2.3	29
9	Using chaotic advection for facile high-throughput fabrication of ordered multilayer micro- and nanostructures: continuous chaotic printing. Biofabrication, 2020, 12, 035023.	7.1	43
10	Biofabrication 2019: Special Issue of Selected Papers from the Annual Meeting of the International Society for Biofabrication. Advanced Healthcare Materials, 2020, 9, e2002049.	7.6	0
11	Influence of Electrical Field Collector Positioning and Motion Scheme on Electrospun Bifurcated Vascular Graft Membranes. Materials, 2019, 12, 2123.	2.9	1
12	Optimization of photocrosslinkable resin components and 3D printing process parameters. Acta Biomaterialia, 2019, 97, 154-161.	8.3	43
13	Modulating Bioglass Concentration in 3D Printed Poly(propylene fumarate) Scaffolds for Post-Printing Functionalization with Bioactive Functional Groups. Biomacromolecules, 2019, 20, 4345-4352.	5.4	17
14	Ceramic coating for delayed degradation of Mg-1.2Zn-0.5Ca-0.5Mn bone fixation and instrumentation. Thin Solid Films, 2019, 687, 137456.	1.8	19
15	Photopolymerizable Resins for 3D-Printing Solid-Cured Tissue Engineered Implants. Current Drug Targets, 2019, 20, 823-838.	2.1	30
16	"Effect of Zn content and aging temperature on the in-vitro properties of heat-treated and Ca/P ceramic-coated Mg-0.5%Ca-x%Zn alloys― Materials Science and Engineering C, 2019, 103, 109700.	7.3	11
17	Poly(propylene fumarate)-based materials: Synthesis, functionalization, properties, device fabrication and biomedical applications. Biomaterials, 2019, 208, 45-71.	11.4	73
18	3D Printing of Poly(propylene fumarate) Oligomers: Evaluation of Resin Viscosity, Printing Characteristics and Mechanical Properties. Biomacromolecules, 2019, 20, 1699-1708.	5.4	93

#	Article	IF	CITATIONS
19	Mechanomics Approaches to Understand Cell Behavior in Context of Tissue Neogenesis, During Prenatal Development and Postnatal Healing. Frontiers in Cell and Developmental Biology, 2019, 7, 354.	3.7	6
20	Bioceramics for Musculoskeletal Regenerative Medicine: Materials and Manufacturing Process Compatibility for Synthetic Bone Grafts and Medical Devices. , 2018, , 161-193.		3
21	Bioceramics for Musculoskeletal Regenerative Medicine: Materials and Manufacturing Process Compatibility for Synthetic Bone Grafts and Medical Devices. , 2018, , 1-33.		1
22	Mechanical evaluation of the SLM fabricated, stiffness-matched, mandibular bone fixation plates. , 2018, , .		1
23	Microstructural, mechanical and corrosion characteristics of heat-treated Mg-1.2Zn-0.5Ca (wt%) alloy for use as resorbable bone fixation material. Journal of the Mechanical Behavior of Biomedical Materials, 2017, 69, 203-212.	3.1	70
24	Design and mechanical characterization of solid and highly porous 3D printed poly(propylene) Tj ETQq0 0 0 rgB1	Overlock	2 19 ₉ Tf 50 542
25	Effect of Chemical and Physical Properties on the In Vitro Degradation of 3D Printed High Resolution Poly(propylene fumarate) Scaffolds. Biomacromolecules, 2017, 18, 1419-1425.	5.4	55
26	Modification of Poly(propylene fumarate)–Bioglass Composites with Peptide Conjugates to Enhance Bioactivity. Biomacromolecules, 2017, 18, 3168-3177.	5.4	24
27	Electrospinning Complexly-shaped, Resorbable, Bifurcated Vascular Grafts. Procedia CIRP, 2017, 65, 207-212.	1.9	12
28	Resorbable bone fixation alloys, forming, and post-fabrication treatments. Materials Science and Engineering C, 2017, 70, 870-888.	7.3	85
29	Fixation Release and the Bone Bandaid: A New Bone Fixation Device Paradigm. Bioengineering, 2017, 4, 5.	3.5	17
30	Finite Element Simulation and Additive Manufacturing of Stiffness-Matched NiTi Fixation Hardware for Mandibular Reconstruction Surgery. Bioengineering, 2016, 3, 36.	3.5	55
31	The Current Role of Three-Dimensional (3D) Printing in Plastic Surgery. Plastic and Reconstructive Surgery, 2016, , 1.	1.4	29
32	The Effect of Heat-Treatment on Mechanical, Microstructural, and Corrosion Characteristics of a Magnesium Alloy With Potential Application in Resorbable Bone Fixation Hardware. , 2016, , .		2
33	On the Effect of Screw Preload on the Stress Distribution of Mandibles During Segmental Defect Treatment Using an Additively Manufactured Hardware. , 2016, , .		2
34	Achieving biocompatible stiffness in NiTi through additive manufacturing. Journal of Intelligent Material Systems and Structures, 2016, 27, 2661-2671.	2.5	58
35	Three Dimensional Printing of Stiffness-tuned, Nitinol Skeletal Fixation Hardware with an Example of Mandibular Segmental Defect Repair. Procedia CIRP, 2016, 49, 45-50.	1.9	48
36	The potential impact of bone tissue engineering in the clinic. Regenerative Medicine, 2016, 11, 571-587.	1.7	65

#	Article	IF	CITATIONS
37	Growth Factor Dose Tuning for Bone Progenitor Cell Proliferation and Differentiation on Resorbable Poly(propylene fumarate) Scaffolds. Tissue Engineering - Part C: Methods, 2016, 22, 904-913.	2.1	19
38	Metals for bone implants: safety, design, and efficacy. Biomanufacturing Reviews, 2016, 1, 1.	4.8	112
39	Metallic Fixation of Mandibular Segmental Defects: Graft Immobilization and Orofacial Functional Maintenance. Plastic and Reconstructive Surgery - Global Open, 2016, 4, e858.	0.6	23
40	Synthesis and Biological Evaluation of Well-Defined Poly(propylene fumarate) Oligomers and Their Use in 3D Printed Scaffolds. Biomacromolecules, 2016, 17, 690-697.	5.4	69
41	Digital micromirror device (DMD)-based 3D printing of poly(propylene fumarate) scaffolds. Materials Science and Engineering C, 2016, 61, 301-311.	7.3	42
42	The Current Role of Three-Dimensional Printing in Plastic Surgery. Plastic and Reconstructive Surgery, 2016, 137, 1045-1055.	1.4	72
43	Process development and characterization of additively manufactured nickel–titanium shape memory parts. Journal of Intelligent Material Systems and Structures, 2016, 27, 2653-2660.	2.5	74
44	Effect of prevascularization on inÂvivo vascularization of poly(propylene fumarate)/fibrin scaffolds. Biomaterials, 2016, 77, 255-266.	11.4	75
45	The Recent Revolution in the Design and Manufacture of Cranial Implants. Neurosurgery, 2015, 77, 814-824.	1.1	89
46	Craniofacial and Dental Tissue. , 2015, , 191-213.		2
47	3D printing of resorbable poly(propylene fumarate) tissue engineering scaffolds. MRS Bulletin, 2015, 40, 119-126.	3.5	69
48	Bioprinting of Bone. , 2015, , 293-308.		5
49	Hydrogels that allow and facilitate bone repair, remodeling, and regeneration. Journal of Materials Chemistry B, 2015, 3, 7818-7830.	5.8	69
50	Evaluating 3Dâ€Printed Biomaterials as Scaffolds for Vascularized Bone Tissue Engineering. Advanced Materials, 2015, 27, 138-144.	21.0	241
51	Validating continuous digital light processing (cDLP) additive manufacturing accuracy and tissue engineering utility of a dye-initiator package. Biofabrication, 2014, 6, 015003.	7.1	53
52	Enhancement of Bone Implants by Substituting Nitinol for Titanium (Ti-6Al-4V): A Modeling Comparison. , 2014, , .		11
53	Modeling and Validation of Additively Manufactured Porous Nitinol Implants. , 2014, , .		4
54	Multiple initiators and dyes for continuous Digital Light Processing (cDLP) additive manufacture of resorbable bone tissue engineering scaffolds. Virtual and Physical Prototyping, 2014, 9, 3-9.	10.4	36

#	Article	IF	CITATIONS
55	Metals for bone implants. Part 1. Powder metallurgy and implant rendering. Acta Biomaterialia, 2014, 10, 4058-4070.	8.3	215
56	Load bearing and stiffness tailored NiTi implants produced by additive manufacturing: a simulation study. Proceedings of SPIE, 2014, , .	0.8	15
57	Evaluation of the In Vitro Cytotoxicity of Cross-Linked Biomaterials. Biomacromolecules, 2013, 14, 1321-1329.	5.4	132
58	Mechanical modulation of nascent stem cell lineage commitment in tissue engineering scaffolds. Biomaterials, 2013, 34, 5766-5775.	11.4	41
59	Dynamic contrast enhanced-magnetic resonance imaging (DCE-MRI) of photodynamic therapy (PDT) outcome and associated changes in the blood-brain barrier following Pc 4-PDT of glioma in an athymic nude rat model. Proceedings of SPIE, 2012, , .	0.8	0
60	Computational Modeling of Tissue Engineering Scaffolds as Delivery Devices for Mechanical and Mechanically Modulated Signals. Studies in Mechanobiology, Tissue Engineering and Biomaterials, 2012, , 127-143.	1.0	3
61	Continuous digital light processing (cDLP): Highly accurate additive manufacturing of tissue engineered bone scaffolds. Virtual and Physical Prototyping, 2012, 7, 13-24.	10.4	108
62	Mapping the Mechanome of Live Stem Cells Using a Novel Method to Measure Local Strain Fields In Situ at the Fluid-Cell Interface. PLoS ONE, 2012, 7, e43601.	2.5	42
63	The influence of stereolithographic scaffold architecture and composition on osteogenic signal expression with rat bone marrow stromal cells. Biomaterials, 2011, 32, 3750-3763.	11.4	133
64	Early osteogenic signal expression of rat bone marrow stromal cells is influenced by both hydroxyapatite nanoparticle content and initial cell seeding density in biodegradable nanocomposite scaffolds. Acta Biomaterialia, 2011, 7, 1249-1264.	8.3	115
65	Stereolithographic Bone Scaffold Design Parameters: Osteogenic Differentiation and Signal Expression. Tissue Engineering - Part B: Reviews, 2010, 16, 523-539.	4.8	209
66	Dynamic contrast enhanced-magnetic resonance imaging (DCE-MRI) for the assessment of Pc 4-sensitized photodynamic therapy of a U87-derived glioma model in the athymic nude rat. Proceedings of SPIE, 2010, , .	0.8	0
67	In Situ Spatiotemporal Mapping of Flow Fields around Seeded Stem Cells at the Subcellular Length Scale. PLoS ONE, 2010, 5, e12796.	2.5	28
68	Effect of Initial Cell Seeding Density on Early Osteogenic Signal Expression of Rat Bone Marrow Stromal Cells Cultured on Cross-Linked Poly(propylene fumarate) Disks. Biomacromolecules, 2009, 10, 1810-1817.	5.4	129
69	Optimal gadolinium dose level for magnetic resonance imaging (MRI) contrast enhancement of U87-derived tumors in athymic nude rats for the assessment of photodynamic therapy. Proceedings of SPIE, 2009, , .	0.8	3
70	Functional Measures of Therapy Based on Radiological Imaging. , 2009, , 427-438.		0
71	Monitoring Pc 4-mediated photodynamic therapy of U87 tumors with dynamic contrast enhanced-magnetic resonance imaging (DCE-MRI) in the athymic nude rat. Proceedings of SPIE, 2008, , .	0.8	1
72	A new Gamma Knife®radiosurgery paradigm: Tomosurgery. Medical Physics, 2007, 34, 1743-1758.	3.0	1

#	Article	IF	CITATIONS
73	Hardware, software, and scanning issues encountered during small animal imaging of photodynamic therapy in the athymic nude rat. , 2007, , .		0
74	Monitoring Pc 4-mediated photodynamic therapy of U87 tumors with 18F- fluorodeoxy-glucose PET imaging in the Athymic Nude Rat. , 2007, , .		2
75	Fluorescence of Pc 4 in U87 cells following photodynamic therapy. , 2007, , .		2
76	Quantifying degeneration of white matter in normal aging using fractal dimension. Neurobiology of Aging, 2007, 28, 1543-1555.	3.1	88
77	A three-dimensional fractal analysis method for quantifying white matter structure in human brain. Journal of Neuroscience Methods, 2006, 150, 242-253.	2.5	95
78	Pc 4 photodynamic therapy of U87 (human glioma) orthotopic tumor in nude rat brain. , 2005, , .		0
79	Surface smoothing and template partitioning for cranial implant CAD. , 2005, , .		1
80	Pc 4 photodynamic therapy of U87-derived human glioma in the nude rat. Lasers in Surgery and Medicine, 2005, 36, 383-389.	2.1	33
81	A Three-Dimensional Morphometric Study of Craniofacial Shape in Schizophrenia. American Journal of Psychiatry, 2005, 162, 606-608.	7.2	41
82	Effect of Transforming Growth Factor β2 on Marrow-Infused Foam Poly(Propylene Fumarate) Tissue-Engineered Constructs for the Repair of Critical-Size Cranial Defects in Rabbits. Tissue Engineering, 2005, 11, 923-939.	4.6	31
83	Effect of biomaterial properties on bone healing in a rabbit tooth extraction socket model. Journal of Biomedical Materials Research Part B, 2004, 68A, 428-438.	3.1	52
84	Use of stereolithography to manufacture critical-sized 3D biodegradable scaffolds for bone ingrowth. Journal of Biomedical Materials Research Part B, 2003, 64B, 65-69.	3.1	451
85	Plug pattern optimization for gamma knife radiosurgery treatment planning. International Journal of Radiation Oncology Biology Physics, 2003, 55, 420-427.	0.8	26
86	Photoinitiated Cross-Linking of the Biodegradable Polyester Poly(propylene fumarate). Part II. In Vitro Degradation. Biomacromolecules, 2003, 4, 1335-1342.	5.4	77
87	Deformable templates for preoperative computer-aided design and fabrication of large cranial implants. International Congress Series, 2003, 1256, 710-715.	0.2	9
88	Photoinitiated Cross-Linking of the Biodegradable Polyester Poly(propylene fumarate). Part I. Determination of Network Structure. Biomacromolecules, 2003, 4, 1327-1334.	5.4	72
89	Poly(propylene fumarate) and Poly(DL-lactic-co-glycolic acid) as Scaffold Materials for Solid and Foam-Coated Composite Tissue-Engineered Constructs for Cranial Reconstruction. Tissue Engineering, 2003, 9, 495-504.	4.6	42
90	Highly Accurate CAD Tools for Cranial Implants. Lecture Notes in Computer Science, 2003, , 99-107.	1.3	6

#	Article	IF	CITATIONS
91	Computer Aided Design of Large-Format Prefabricated Cranial Plates. Journal of Craniofacial Surgery, 2003, 14, 819-832.	0.7	111
92	Effect of Changing Patient Position from Supine to Prone on the Accuracy of a Brown-Roberts-Wells Stereotactic Head Frame System. Neurosurgery, 2003, 52, 610-618.	1.1	33
93	Integration of Neurosurgical Image Guidance and an Intraoperative Magnetic Resonance Scanner. Stereotactic and Functional Neurosurgery, 2003, 80, 136-139.	1.5	4
94	Use of stereolithography to manufacture critical-sized 3D biodegradable scaffolds for bone ingrowth. , 2003, 64B, 65.		1
95	<title>Effect of changing patient position from supine to prone on the accuracy of a
Cosman-Roberts-Wells (CRW) stereotactic head frame system</title> . , 2002, 4681, 516.		0
96	In vitro degradation and fracture toughness of multilayered porous poly(propylene) Tj ETQq0 0 0 rgBT /Overlock 1 159-164.	0 Tf 50 54 3.1	17 Td (fuma 27
97	Bone formation in transforming growth factor ?-1-coated porous poly(propylene fumarate) scaffolds. Journal of Biomedical Materials Research Part B, 2002, 60, 241-251.	3.1	106
98	Soft and hard tissue response to photocrosslinked poly(propylene fumarate) scaffolds in a rabbit model. Journal of Biomedical Materials Research Part B, 2002, 59, 547-556.	3.1	230
99	Photocrosslinking characteristics and mechanical properties of diethyl fumarate/poly(propylene) Tj ETQq1 1 0.784	314 rgBT 11.4	/Overlock
100	Photoinitiated Polymerization of Biomaterials. Annual Review of Materials Research, 2001, 31, 171-181.	9.3	147
101	Synthesis and properties of photocross-linked poly(propylene fumarate) scaffolds. Journal of Biomaterials Science, Polymer Edition, 2001, 12, 673-687.	3.5	162
102	Three-dimensional imaging: The caseWestern Reserve University method. Seminars in Orthodontics, 2001, 7, 233-243.	1.4	3
103	Optimization of Gamma Knife treatment planning via guided evolutionary simulated annealing. Medical Physics, 2001, 28, 1746-1752.	3.0	27
104	Medial Axis Seeding of a Guided Evolutionary Simulated Annealing (GESA) Algorithm for Automated Gamma Knife Radiosurgery Treatment Planning. Lecture Notes in Computer Science, 2001, , 441-448.	1.3	0
105	Three-Dimensional Bolton–Brush Growth Study Landmark Data: Ontogeny and Sexual Dimorphism of the Bolton Standards Cohort. Cleft Palate-Craniofacial Journal, 2000, 37, 145-156.	0.9	34
106	The brush inquiry: An opportunity to investigate health outcomes in a well-characterized cohort. , 2000, 12, 1-9.		31
107	A procedure to average 3D anatomical structures. Medical Image Analysis, 2000, 4, 317-334.	11.6	13
108	Statistical Shape Analysis. Journal of Human Evolution, 2000, 38, 455-457.	2.6	3

#	Article	IF	CITATIONS
109	Fast verification of Gamma Knifeâ,,¢ treatment plans. Journal of Applied Clinical Medical Physics, 2000, 1, 158-164.	1.9	12
110	Three-Dimensional Bolton–Brush Growth Study Landmark Data: Ontogeny and Sexual Dimorphism of the Bolton Standards Cohort. Cleft Palate-Craniofacial Journal, 2000, 37, 145-156.	0.9	23
111	Fast verification of Gamma Knifeâ"¢ treatment plans. Journal of Applied Clinical Medical Physics, 2000, 1, 158.	1.9	15
112	Local Integration of Commercially Available Intra-operative MR-scanner and Neurosurgical Guidance for Metalloporphyrin-Guided Tumor Resection and Photodynamic Therapy. Lecture Notes in Computer Science, 2000, , 338-347.	1.3	1
113	Three-dimensional magnetic resonance-based morphometrics and ventricular dysmorphology in schizophrenia. Biological Psychiatry, 1999, 45, 62-67.	1.3	31
114	Osseointegration of Preformed Polymethylmethacrylate Craniofacial Prostheses Coated with Bone Marrow-Impregnated Poly (DL-Lactic-co-Glycolic Acid) Foam. Plastic and Reconstructive Surgery, 1999, 104, 705-712.	1.4	17
115	Osseointegration of Preformed Polymethylmethacrylate Craniofacial Prostheses Coated with Bone Marrow-Impregnated Poly (DL-Lactic-co-Glycolic Acid) Foam. Plastic and Reconstructive Surgery, 1999, 104, 705-712.	1.4	28
116	Mammalian fauna and biostratigraphy of the pre-Neandertal site of Reilingen, Germany. Journal of Human Evolution, 1998, 34, 469-484.	2.6	15
117	On the phylogenetic position of the pre-Neandertal specimen from Reilingen, Germany. Journal of Human Evolution, 1998, 34, 485-508.	2.6	162
118	Validation of object-induced MR distortion correction for frameless stereotactic neurosurgery. IEEE Transactions on Medical Imaging, 1998, 17, 810-816.	8.9	24
119	Average African American Three-Dimensional Computed Tomography Skull Images. Journal of Craniofacial Surgery, 1998, 9, 348-358.	0.7	19
120	<title>Accuracy and precision of 3D cephalometric landmarks from biorthogonal plain-film x rays</title> ., 1998,,.		1
121	<title>New 3D Bolton standards: coregistration of biplane x rays and 3D CT</title> . , 1997, , .		0
122	<title>Scanned bi-orthogonal radiographs as a source for 3D cephalometric data</title> . , 1996, 2710, 717.		4
123	Three dimensional MR-based morphometric comparison of schizophrenic and normal cerebral ventricles. Lecture Notes in Computer Science, 1996, , 361-372.	1.3	20
124	Chi-Square Test of Biological Space Curve Affinities. , 1996, , 235-251.		5
125	A Three-Dimensional Smooth Surface Analysis of Untreated Crouzon's Syndrome in the Adult. Journal of Craniofacial Surgery, 1995, 6, 444-453.	0.7	37
126	Homo at the gates of Europe. Nature, 1995, 373, 472-473.	27.8	28

#	Article	IF	CITATIONS
127	Features of the Dmanisi mandible. Nature, 1995, 373, 473-473.	27.8	1
128	Reconstruction of human fossils. IEEE Computer Graphics and Applications, 1995, 15, 12-15.	1.2	24
129	Morphometrics and Michaelangelo. Journal of Human Evolution, 1994, 27, 457-460.	2.6	1
130	<title>The wrapper: a surface optimization algorithm that preserves highly curved areas</title> . , 1994, 2359, 631.		13
131	<title>Spline-based approach for averaging three-dimensional curves and surfaces</title> . , 1993, 2035, 29.		13
132	Vocal grooming: Man the schmoozer. Behavioral and Brain Sciences, 1993, 16, 699-700.	0.7	79
133	Second gorilla or third chimp?. Nature, 1992, 359, 676-677.	27.8	49
134	Quantitative and qualitative comparison of volumetric and surface rendering techniques. IEEE Transactions on Nuclear Science, 1991, 38, 659-662.	2.0	17
135	Optimization of Photocrosslinkable Resin Components and 3D Printing Process Parameters. SSRN Electronic Journal, 0, , .	0.4	0